Sheet Forming Simulations of Automotive Parts using Different Yield Functions

Jin-Woo Lee, Frédéric Barlat, and Dong-Jin Kim

Citation: AIP Conference Proceedings **1252**, 361 (2010); doi: 10.1063/1.3457575
View online: http://dx.doi.org/10.1063/1.3457575
View Table of Contents: http://scitation.aip.org/content/aip/proceeding/aipcp/1252?ver=pdfcov
Published by the AIP Publishing

Articles you may be interested in

Two-surface plasticity Model and Its Application to Spring-back Simulation of Automotive Advanced High Strength Steel Sheets
AIP Conf. Proc. **1383**, 1175 (2011); 10.1063/1.3623736

An evolutionary yield function based on Barlat 2000 yield function for the superconducting niobium sheet
AIP Conf. Proc. **1383**, 210 (2011); 10.1063/1.3623613

Finite element simulation of sheet metal forming and springback using a crystal plasticity approach
AIP Conf. Proc. **908**, 769 (2007); 10.1063/1.2740903

Finite Element Simulation of Sheet Metal Forming Using Anisotropic Strain-Rate Potentials
AIP Conf. Proc. **908**, 643 (2007); 10.1063/1.2740883

Impact of the Parameter Identification of Plastic Potentials on the Finite Element Simulation of Sheet Metal Forming
AIP Conf. Proc. **907**, 327 (2007); 10.1063/1.2729533

This article is copyrighted as indicated in the article. Reuse of AIP content is subject to the terms at: http://scitation.aip.org/termsconditions. Downloaded to IP: 141.223.153.212 On: Mon, 14 Dec 2015 09:06:25

Sheet Forming Simulations of Automotive Parts using Different Yield Functions

Jin-Woo Lee[a], Frédéric Barlat [a] and Dong-Jin Kim[b]

[a]*Graduate Institute of Ferrous Technology, Pohang University of Science and Technology, San 31 Hyoja-Dong, Nam-Gu, Pohang, Gyeongbuk 790-784, Republic of Korea*
[b]*Automotive Steel Applications Research Group, POSCO, Kumho-Dong, Gwangyang,Cheonnam,545-875, Republic of Korea*

Abstract. In this work, the influence of the yield function on finite element (FE) forming simulation results for two auto-body panels, hood inner and door outer, was investigated. Simulations were conducted with different yield functions, Hill's1948, Yld91 and Yld2000-2d, which are available in the PAM-STAMP and LS-DYNA commercial codes. Although moderate, some differences in the results were observed.

Keywords: Yield function, constitutive model, sheet forming simulations, finite element method
PACS: 62.20.fq

INTRODUCTION

Today, forming process simulations of automotive components are used quite intensively in the design stage of a vehicle's development. Numerical analyses are important in order to understand the complex deformation mechanics that occurs during sheet forming processes. With finite element (FE) codes, it is possible to find the areas where problems, such as plastic flow localization, fracture, wrinkling and springback are likely to arise during a real forming operation. In order to optimize the process, it is necessary to obtain a precise estimate of the occurrence of the different failure modes. However, failure depends on the constitutive models used in the simulations.

Most industrial sheet metal forming simulations are performed using a phenomenological constitutive description for the elasto-plastic material behavior. The material is often assumed to be isotropic since plastic anisotropy theories and their implementations in FE codes lead to additional difficulties and computation time. Moreover, extra test results are necessary to identify all the material coefficients. In this work, the plastic behavior is assumed to be well described with a yield function, the associated flow rule and a hardening law. The latter is assumed to be strain rate insensitive and temperature independent. A range of different material parameters could be investigated but the objective of this work was to compare the simulation results using different yield functions, i.e., Hill [1], Yld91 [2], and Yld2000-2d [3]. Forming of automotive inner and outer panels were simulated using the commercial codes PAM-STAMP and LS-DYNA, respectively.

YIELD FUNCTIONS FOR ANISOTROPIC MATERIALS

The primary cause of anisotropy of plastic properties is crystallographic texture. Mechanical working, i.e., the rolling process, makes materials have preferred grain orientations. Over the last decades, anisotropic yield functions, which were consistent with crystal plasticity calculations, were proposed. Two of these formulations are considered in this work. In addition, Hill's 1948 yield function was used as a reference for comparison.

This article is copyrighted as indicated in the article. Reuse of AIP content is subject to the terms at: http://scitation.aip.org/termsconditions. Downloaded to IP: 141.223.153.212 On: Mon, 14 Dec 2015 09:06:25

Hill's 1948 Yield Function

Hill [1] proposed the following yield function for anisotropic materials exhibiting orthotropic symmetry such as rolled sheets and plates. This yield function has been widely used in analytical works dealing with plastic anisotropy and in numerical simulations of forming processes for anisotropic materials. The formulation is valid for a general stress state. However, a plane stress state is very often assumed for practical sheet forming applications and Hill's 1948 yield criterion reduces to

$$\phi = F\sigma_{yy}{}^2 + G\sigma_{xx}{}^2 + H(\sigma_{xx} - \sigma_{yy})^2 + 2N\sigma_{xy}^2 = \bar{\sigma}^2 \tag{1}$$

In this equation, *F*, *G*, *H*, and *N* are the anisotropy coefficients, and $\bar{\sigma}$ is the equivalent stress. In order to calibrate the equivalent stress on the flow stress-strain curve in a particular direction, a relationship between the coefficients is established. For instance, if the equivalent stress is calibrated on the stress-strain curve in the rolling direction (RD or **x**), then $\sigma_{xx} = \sigma_0$ is the only non-zero stress component and the relationship $G + H = 1$ follows. The other coefficients can be calculated using either the r values (width-to-thickness strain ratio of tension specimen) measured in three different directions of the sheet, i.e., r_0, r_{45} and r_{90}, or three yield stresses different from σ_0.

Yld91 yield function

For this case, the yield function ϕ is generally defined as

$$\phi = \left|\tilde{S}_1 - \tilde{S}_2\right|^m + \left|\tilde{S}_2 - \tilde{S}_3\right|^m + \left|\tilde{S}_3 - \tilde{S}_1\right|^m = 2\bar{\sigma}^m \tag{2}$$

where $\tilde{S}_{i=1,2,3}$ are the principal values of the symmetric tensor $\tilde{S}_{\alpha\beta}$

$$\left[\tilde{\mathbf{S}}\right] = \begin{bmatrix} \left[c\left(\sigma_{xx} - \sigma_{yy}\right) - b\left(\sigma_{zz} - \sigma_{xx}\right)\right]/3 & h\sigma_{xy} & g\sigma_{zx} \\ h\sigma_{xy} & \left[a\left(\sigma_{yy} - \sigma_{zz}\right) - c\left(\sigma_{xx} - \sigma_{yy}\right)\right]/3 & f\sigma_{yz} \\ g\sigma_{zx} & f\sigma_{yz} & \left[b\left(\sigma_{zz} - \sigma_{xx}\right) - a\left(\sigma_{yy} - \sigma_{zz}\right)\right]/3 \end{bmatrix} \tag{3}$$

The material constants *a*, *b*, *c*, *f*, *g* and *h* are the anisotropy coefficients. When *a*=*b*=*c*=*f*=*g*=*h*=1, the material is isotropic and the yield surface reduces to the Tresca yield surface for *a*=1 or ∞ and von Mises yield surface for *a*=2 or 4. Moreover, *a*=6 and *a*=8 are recommended values for body centered cubic (BCC) and face centered cubic (FCC) materials, respectively. As for Hill's yield function, four coefficients are available for the plane stress case ($\sigma_{yz} = \sigma_{zx} = \sigma_{zz} = 0$) and can be calculated with the same input data.

Yld2000-2d yield function

This yield function ϕ is formulated for the case of the plane stress. It is defined as

$$\begin{aligned} &\phi = \phi' + \phi'' = 2\bar{\sigma}^m \\ &\phi' = \left|\tilde{S}_1' - \tilde{S}_2'\right|^m, \quad \phi'' = \left|2\tilde{S}_2'' + \tilde{S}_1''\right|^m + \left|2\tilde{S}_1'' + \tilde{S}_2''\right|^m \end{aligned} \tag{4}$$

The $\tilde{S}_i'$ and $\tilde{S}_i''$ are the principal values of $\tilde{s}_{ij}'$ and $\tilde{s}_{ij}''$, which can be expressed in the following form

$$\tilde{S}_{1,2} = \frac{1}{2}\left(\tilde{s}_{xx} + \tilde{s}_{yy} \pm \sqrt{\left(\tilde{s}_{xx} - \tilde{s}_{yy}\right)^2 + 4\tilde{s}_{xy}^2}\right) \tag{5}$$

This article is copyrighted as indicated in the article. Reuse of AIP content is subject to the terms at: http://scitation.aip.org/termsconditions. Downloaded to IP: 141.223.153.212 On: Mon, 14 Dec 2015 09:06:25

with the appropriate "prime" and "double prime" for each stress. The s'_{ij} and s''_{ij} are linear functions of the stress deviator, i.e.,

$$\begin{pmatrix} s'_{xx} \\ s'_{yy} \\ s'_{xy} \end{pmatrix} = \begin{bmatrix} L'_{11} & L'_{12} & 0 \\ L'_{21} & L'_{22} & 0 \\ 0 & 0 & L'_{66} \end{bmatrix} \begin{pmatrix} s_{xx} \\ s_{yy} \\ s_{xy} \end{pmatrix} \quad \begin{pmatrix} s''_{xx} \\ s''_{yy} \\ s''_{xy} \end{pmatrix} = \begin{bmatrix} L''_{11} & L''_{12} & 0 \\ L''_{21} & L''_{22} & 0 \\ 0 & 0 & L''_{66} \end{bmatrix} \begin{pmatrix} s_{xx} \\ s_{yy} \\ s_{xy} \end{pmatrix} \tag{6}$$

In turn, the coefficients L'_{ij} and L''_{ij} can be expressed with a set of eight coefficients α_k

$$\begin{pmatrix} L'_{11} \\ L'_{12} \\ L'_{21} \\ L'_{22} \\ L'_{66} \end{pmatrix} = \begin{bmatrix} 2/3 & 0 & 0 \\ -1/3 & 0 & 0 \\ 0 & -1/3 & 0 \\ 0 & 2/3 & 0 \\ 0 & 0 & 1 \end{bmatrix} \begin{pmatrix} \alpha_1 \\ \alpha_2 \\ \alpha_7 \end{pmatrix} \quad \begin{pmatrix} L''_{11} \\ L''_{12} \\ L''_{21} \\ L''_{22} \\ L''_{66} \end{pmatrix} = \frac{1}{9} \begin{bmatrix} -2 & 2 & 8 & -2 & 0 \\ 1 & -4 & -4 & 4 & 0 \\ 4 & -4 & -4 & 4 & 0 \\ -2 & 8 & 2 & -2 & 0 \\ 0 & 0 & 0 & 0 & 9 \end{bmatrix} \begin{pmatrix} \alpha_3 \\ \alpha_4 \\ \alpha_5 \\ \alpha_6 \\ \alpha_8 \end{pmatrix} \tag{7}$$

All the coefficients α_k (for *k* form 1 to 8) reduce to 1 in the isotropic case. All these coefficients are independent. This means that eight input data are needed for their identification. Both r values and yield stresses in three directions, i.e., r_0, r_{45}, r_{90}, σ_0, σ_{45}, and σ_{90} from uniaxial tension tests are used. Two additional test results are needed to identify all the α_k coefficients. For instance, these can be provided by the bulge and the disk compression tests [3]. Assumptions must be made if some of these test results are not available (see below).

MATERIALS

Finite element simulations were carried out for two materials, DQIF (deep drawing interstitial free) and 340BH (bake hardenable) steel sheets. DQIF steel sheets are most widely used for automotive parts, especially for rear floor or side body outer panels, which require high formability. In this work, the properties of a DQIF steel sheet sample were used for the simulation of a hood inner panel. For this material, only the RD hardening curve and the experimental r values measured in three directions were available (see Table 1). The four anisotropic coefficients of Hill's 1948 were calculated from a closed form solution, while those of Yld91 were computed using the Newton-Raphson iteration method. The resulting anisotropic coefficients are summarized in Table 2. Figure 1.a shows the corresponding yield loci. Although the input data for these two models are the same, a large difference in yield locus can be observed near balanced biaxial tension. The stress-strain behavior of DQIF was described by the Swift law

$$\bar{\sigma} = 614\left(0.008 + \bar{\varepsilon}\right)^{0.2} \qquad \text{(MPa)} \tag{8}$$

TABLE 1. Material Mechanical Property for DQ steel.

	r_0	r_{45}	r_{90}
DQ steel	1.98	1.48	2.48

TABLE 2. Exponent and anisotropy coefficients of Hill's 1948 and Yld 91 for DQIF steel sheet sample.

	F	G	H	N		
	0.268	0.336	0.664	1.195		
m	a	b	c	f	g	h
6	0.799	0.859	1.131	0.919	0.772	0.758

This article is copyrighted as indicated in the article. Reuse of AIP content is subject to the terms at: http://scitation.aip.org/termsconditions. Downloaded to IP: 141.223.153.212 On: Mon, 14 Dec 2015 09:06:25

TABLE 3. Material Mechanical Property for 340BH steel.

	Yield Stress(MPa)	r value
0°	244.4	1.41
45°	268.0	1.32
90°	248.6	1.62

TABLE 4. The exponent and anisotropy coefficients of Hill's 1948 and Yld2000-2d for 340BH steel.

	F	G	H	N				
	0.268	0.336	0.664	1.195				
m	α_1	α_2	α_3	α_4	α_5	α_6	α_7	α_8
6	1.045	1.012	1.050	0.963	0.983	1.057	0.946	0.737

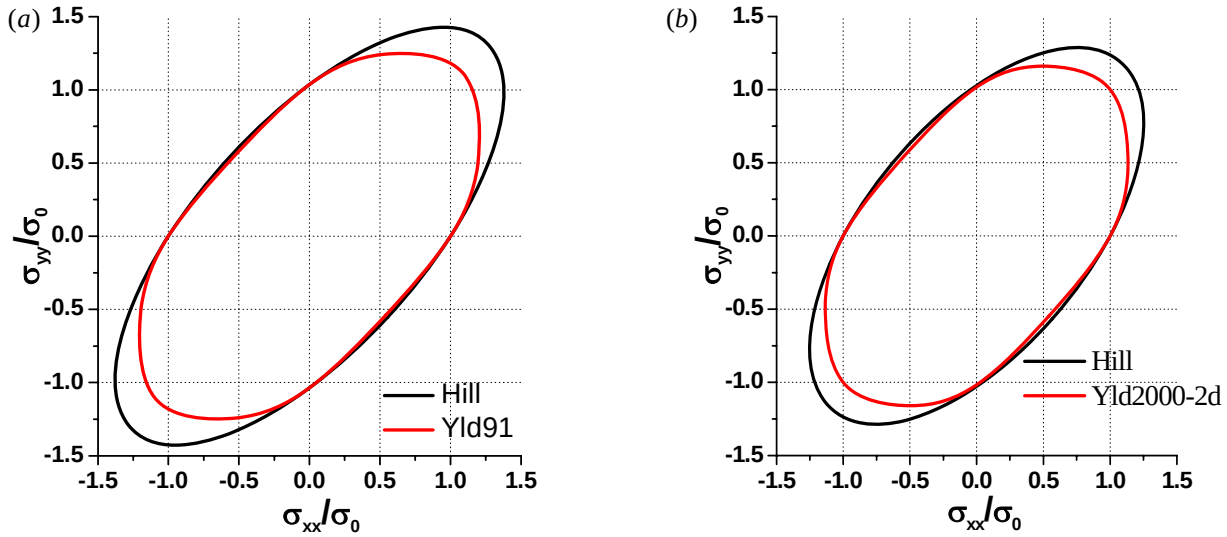

FIGURE 1. Yield loci normalized by the rolling direction uniaxial yield stress (a) DQIF Steel (b) 340BH Steel.

Bake Hardenable (BH) steels are designed and manufactured with the proper interstitial element content so that their yield strength increases after paint baking. These steels can be deformed easily during the initial forming stage after which their yield strength increases by more than 30MPa with the "bake hardening effect". Compared to conventional steel, BH steels have better dent resistance and, therefore, can be used with a smaller gauge for similar performance. This steel is widely employed for body panels, which requires better dentability and higher formability, such as hoods and door outer panels. In this work, simulations were carried out on a 340BH steel sample for a door outer panel. For this material, uniaxial tension tests in three different directions were conducted. The corresponding r values and yield stresses are listed in Table 3. Yld91 and Yld2000-2d yield function were identified and the anisotropy coefficients are summarized in Table 4. For the latter, since the bulge test was not conducted, it was assumed that the flow stress in balanced biaxial tension was the same as that for uniaxial tension in the RD. The balanced biaxial r value, r_b [3], was computed using another yield function (Yld96) [4]. The corresponding yield loci are shown in Fig. 1.b.

NUMERICAL ANALYSIS

Process parameters

Figure 2.a and 2.b represent the hood inner and door outer panels, respectively. The forming process parameters are given in Table 5. It is worth noting that PAM-STAMP generates the entire forming limit diagram based on the strain hardening exponent (n) and gauge (t) using Keeler and Brazier's formula for plane strain [5]

This article is copyrighted as indicated in the article. Reuse of AIP content is subject to the terms at: http://scitation.aip.org/termsconditions. Downloaded to IP: 141.223.153.212 On: Mon, 14 Dec 2015 09:06:25

$$FLD_0 = n(1+0.72t) \quad (n \le 0.2) \quad \text{and} \quad FLD_0 = 0.2(1+0.72t) \quad (n \ge 0.2)$$

An adaptive mesh technique with four refinement levels was adopted, which leads to a mesh of about 1 mm in the most deformed regions at the end of the simulations.

RESULTS AND DISCUSSIONS

Figure 3 shows qualitatively the forming performance for the hood inner panel as predicted with PAM-STAMP using Hill and Yld91 yield functions. Although the trends are similar with the two yield functions, the code does not detect a crack with Hill yield function (Fig. 3a). In contrast, a crack region (circle) was obtained with the Yld91 yield function (Fig. 3b). The strain distribution in all the panel elements can be compared with the approximate forming limit curve (FLD) calculated in PAM-STAMP (Fig. 4). Two points are above the forming limit diagram in Fig. 4b, i.e., with the simulations using Yld91. Of course, this analysis is qualitative and a better quantitative assessment can be obtained by representing a strain profile along a critical cross-section of the panel. For instance, Fig.5 shows the thickness strain distribution along the cross-section AB depicted in Fig. 3. This figure shows that thinning is virtually the same excepted for the position at about 200mm from point A, for which the maximum

TABLE 5. FE Analysis Condition.

	Die Speed	Blank Holder Force	Drawbead Force	Friction Coefficient	Initial Element Size
Hood Inner Panel	5 m/s	600 kN	Ft=0.04kN/mm Fn=0.28kN/mm	0.12	8mm X 8mm
Door Outer Panel	5 m/s	1200 kN	Ft=0.2kN/mm Fn=0.18kN/mm	0.15	15.9mm X 15.7mm

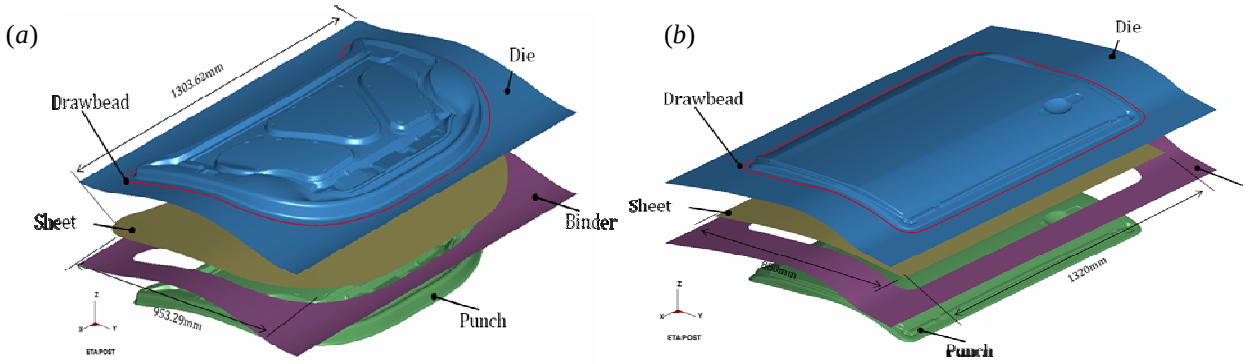

FIGURE 2. Forming models: (a) Hood inner panel (b) Door outer panel.

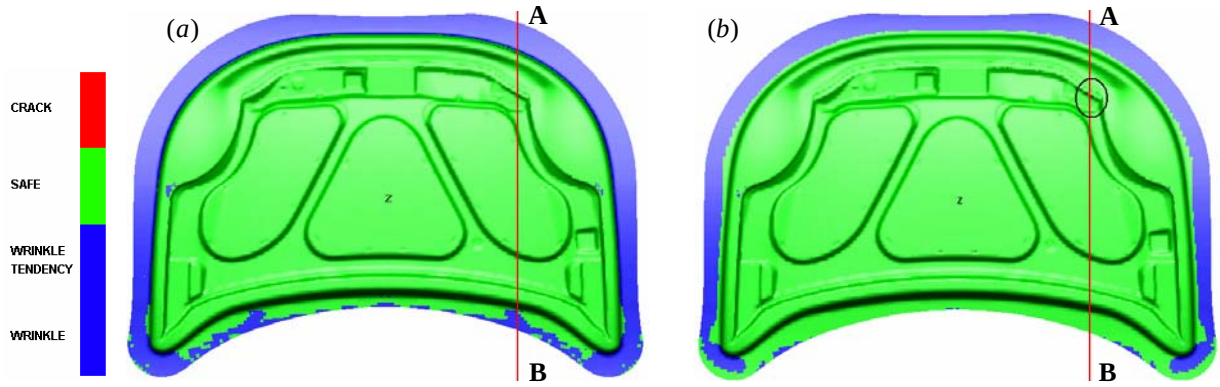

FIGURE 3. The qualitative major strain distribution using PAM-STAMP (a) Hill yield function (b) Yld91 yield function.

This article is copyrighted as indicated in the article. Reuse of AIP content is subject to the terms at: http://scitation.aip.org/termsconditions. Downloaded to IP: 141.223.153.212 On: Mon, 14 Dec 2015 09:06:25

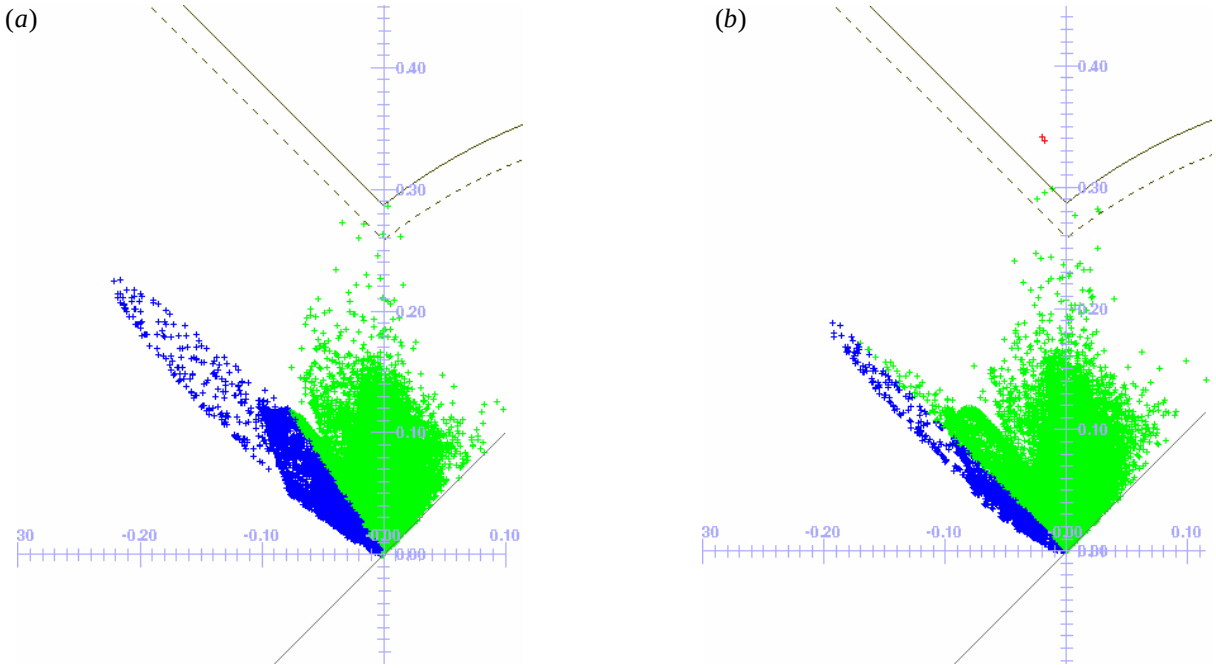

FIGURE 4. Strain distribution of hood inner panel using PAM-STAMP (a) Hill yield function (b) Yld91 yield function.

thickness strain difference predicted with the two yield functions is about 15%. This is a significant difference, particularly because it is located in one of the most critical area. Therefore, it can be concluded that the choice of the yield function has an influence on the results. A more refined analysis is still required because for this particular area, the mesh size of 1mm is, perhaps, too coarse. Moreover, a bending mode of deformation is also involved in this area, which cannot be analyzed simply with the FLD concept. Finally, strain rate sensitivity, which is known to affect strain distribution significantly, should be accounted for in the model.

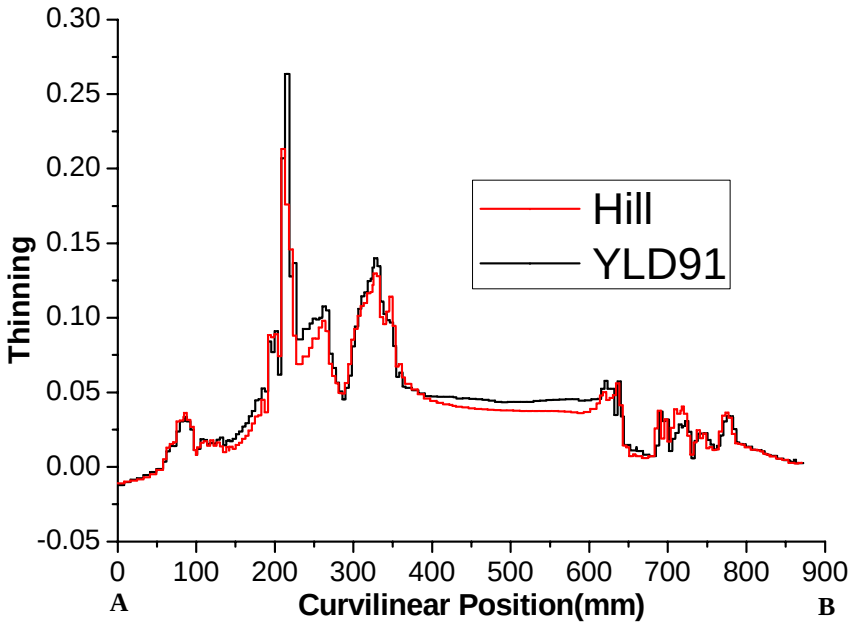

FIGURE 5. Thinning distribution along Cross-Section A-B in Fig. 3.

This article is copyrighted as indicated in the article. Reuse of AIP content is subject to the terms at: http://scitation.aip.org/termsconditions. Downloaded to IP: 141.223.153.212 On: Mon, 14 Dec 2015 09:06:25

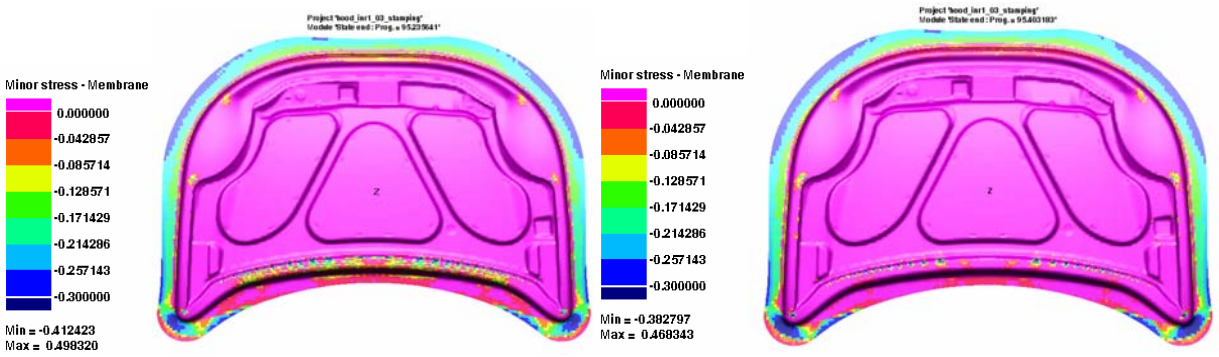

FIGURE 6. The minor stress distribution using Pam-Stamp (a) Hill Yield Criterion (b) Yld 91 Yield Criterion.

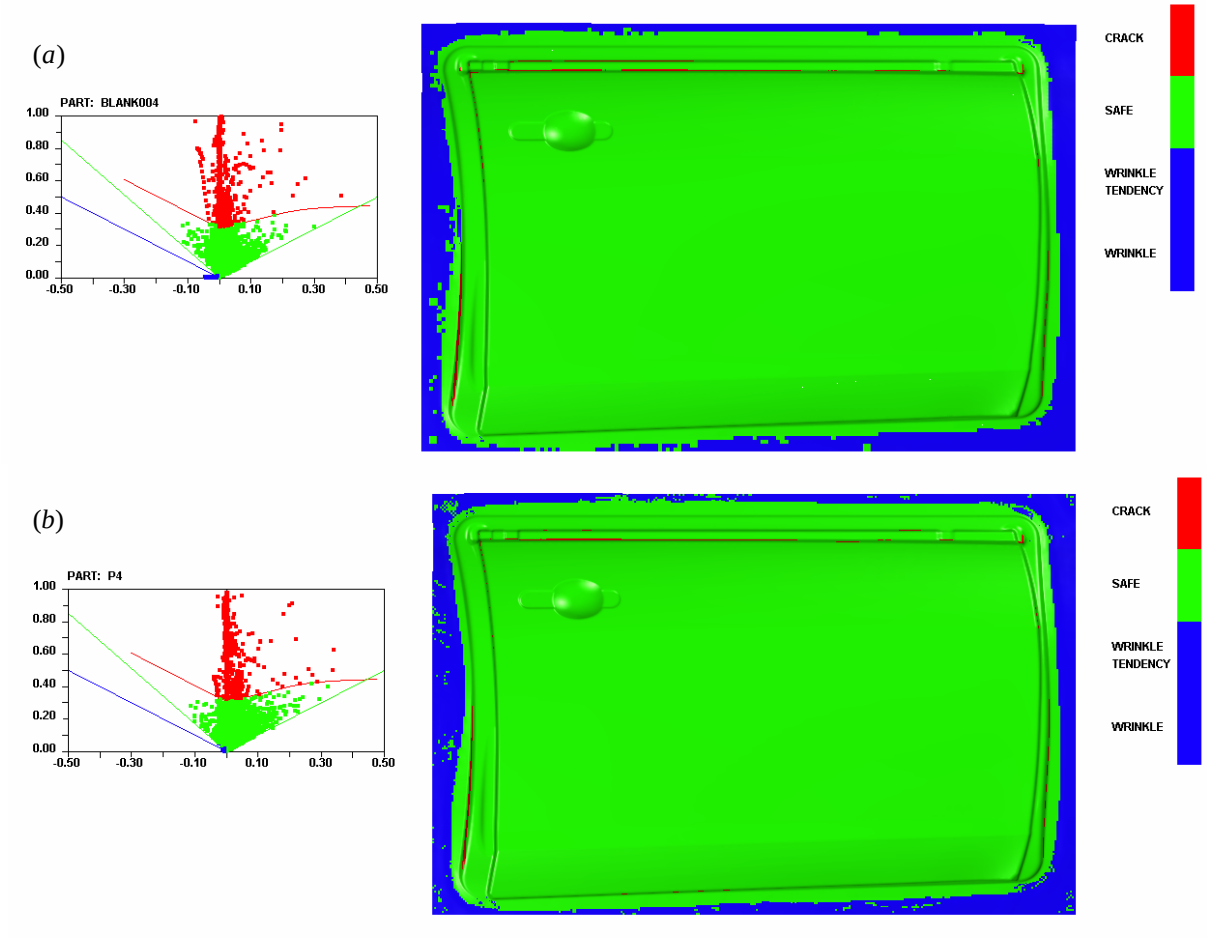

FIGURE 7. The forming limit diagram using LS-DYNA (a) Hill yield function (b) Yld2000-2d yield function.

In Fig. 4, points with minor strains such that $|\varepsilon_{\text{minor}}| \geq |\varepsilon_{\text{major}}| (\varepsilon_{\text{minor}} \leq 0, \varepsilon_{\text{major}} \geq 0)$ were predicted with both yield functions. Depending on the geometry, areas containing these large negative strains could be subjected to wrinkling. Figure 4 indicates that both yield functions leads to essentially the same results in terms of wrinkling tendency. This result is not surprising based on the inspection of the associated yield loci in Fig. 1a. These strains correspond to the right lower quadrant where both yield loci are identical. Figure 6 shows the minor stress distribution and as expected, no major difference can be observed.

This article is copyrighted as indicated in the article. Reuse of AIP content is subject to the terms at: http://scitation.aip.org/termsconditions. Downloaded to IP: 141.223.153.212 On: Mon, 14 Dec 2015 09:06:25

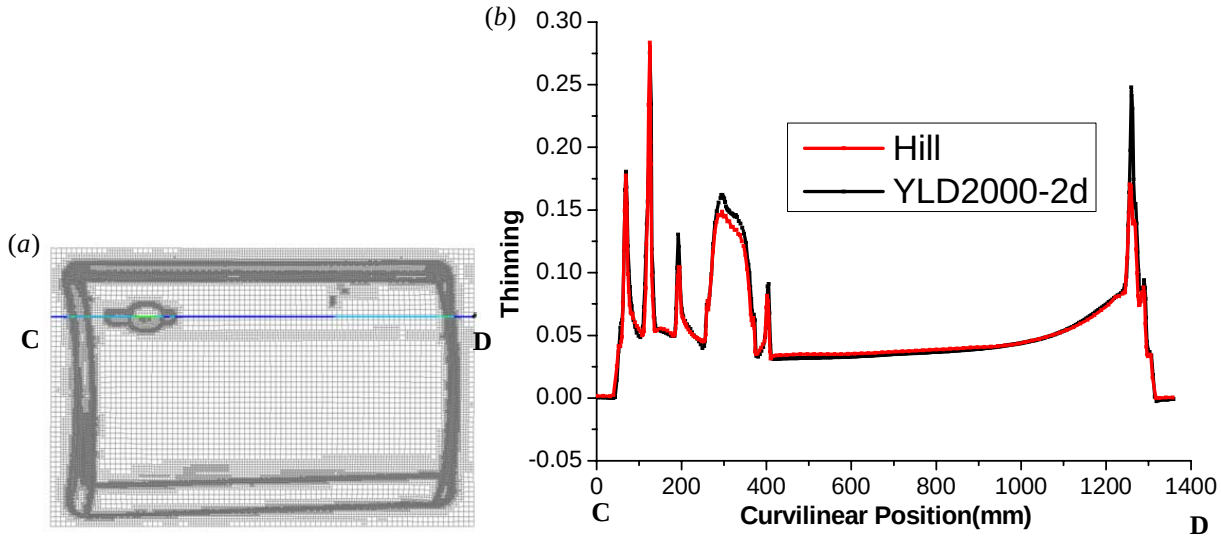

FIGURE 8. (a) Section cut (b) Thinning distribution along section cut.

Figure 7 shows the differences in the forming performance for the door outer panel as calculated with LS-DYNA using Hill and Yld2000-2d yield functions. Many cracks as defined by the software can be detected with both yield functions. Figure 8 shows the thinning distribution along the cross-section CD in Fig. 7. Again, in general, thinning is virtually the same for this type of constrained deformation, except in the critical areas. For instance, near the door handle, the strain predicted with Yld2002-2d is about 10% larger than that predicted with Hill's 1948. Moreover, the maximum strain in the panel is about 25% larger than that predicted with Hill's 1948. Again, at this point, a finer analysis is necessary because of the issues already discussed in the previous example.

CONCLUSIONS

FE forming simulations of two automotive panels were conducted using commercial codes PAM-STAMP and LS-DYNA. Two different yield functions were used for each of the two examples. Based on the standard output from the commercial codes, the yield function does not seem to influence the results significantly. However, with a closer look, up to 25% difference in maximum thickness strains were computed in the critical areas of the panels. Since the success of an operation depends on these critical areas, it can be concluded that the choice of a yield function is important. Moreover, issues related to the mesh size, the material behavior, the deformation mode and the failure behavior requires an even more comprehensive analysis.

ACKNOWLEDGMENTS

The authors are grateful to POSCO for providing material data and CAD files, and for financial support.

REFERENCES

1. R. Hill, *Proceedings of Royal Society of London* **193**, 281-297 (1948).
2. F. Barlat, D.J. Lege and J.C. Brem, *International Journal of Plasticity* **7**, 693-712 (1991).
3. F. Barlat et al., *International Journal of Plasticity* **19**, 1297-1319 (2003).
4. F. Barlat et al., *Journal of the Mechanics and Physics of Solids* . **45**, 1727-1763 (1997).
5. S. P. Keeler and W. G. Brazier, Relationship Between Laboratory Material Characterization and Press-Shop Formability, in *Microalloying 75*, Union Carbide, 1977, pp. 517-528.

This article is copyrighted as indicated in the article. Reuse of AIP content is subject to the terms at: http://scitation.aip.org/termsconditions. Downloaded to IP: 141.223.153.212 On: Mon, 14 Dec 2015 09:06:25